Hindawi
Geofluids
Volume 2022, Article ID 4510194, 10 pages
https://doi.org/10.1155/2022/4510194

Research Article

Study on the Influence Rule of High-Pressure Water Jet Nozzle Parameters on the Effect of Hydraulic Slotting

Beifang Gu[1], **Ruili Hu**[2], **Longkang Wang**[3] and **Guanchao Xu**[1]

[1]*School of Environmental and Municipal Engineering, North China University of Water Resources and Electric Power, Zhengzhou, Henan, China*
[2]*University of International Business and Economics, Beijing, China*
[3]*China Center for Information Industry Development, Beijing, China*

Correspondence should be addressed to Beifang Gu; 289187395@qq.com and Longkang Wang; wlkmit@163.com

Received 21 May 2022; Accepted 27 July 2022; Published 20 August 2022

Academic Editor: Yingfeng Sun

In order to get the appropriate nozzle parameters, numerical simulation and field tests are used to investigate the influence of high-pressure water jet nozzle parameters on the effect of hydraulic slotting. A nozzle model is created by using FLUENT software. For different nozzle contraction angles, outlet diameters, and straight column section lengths, the distribution rules of the velocity of the water jet and dynamic pressure on the central and vertical axes are obtained, and the parameters for the best nozzle effect are determined. The relationship between the nozzle contraction angle gradient, the inlet water pressure, and the nozzle outlet water velocity is discovered. A mathematical model of the nozzle outlet water velocity of the water jet is established. The depth, width, and volume of the hole generated by the nozzle impact are employed as indications for inquiry, and field measurements are used to derive the results of nozzle geometry parameter optimization. The field tests validate the numerical simulation conclusions, and the results have theoretical and practical guidance for hydraulic slotting in coal mines and get the appropriate nozzle parameters specially.

1. Introduction

Hydraulic slotting is an effective method of increasing the permeability of coal seams, and many scholars have studied the high-pressure water jets used for this measure. Yang et al. [1] studied two different structures of conical nozzles and performed numerical simulations based on fluid mechanics knowledge for the parameters of flow field pressure, velocity, and medium of the nozzles, and the advantages and disadvantages of these two nozzles are also compared in detail. Ma and Zhang [2] established a three-dimensional mathematical model of the internal flow field of the nozzle used for soil reaming using numerical simulation software and analyzed the effects of nozzle parameter changes on the velocity distribution, pressure distribution, and outlet velocity of the flow field. Zhang et al. [3] investigated the nozzle modeling and the effect of nozzle parameters by a numerical simulation method. By researching the acceleration mechanism of the water jet within the nozzle, Ge et al. [4] concluded that the length-to-diameter ratio has a large effect on the nozzle outlet jet velocity and performed numerical simulations. Based on Hashish cutting theory, Zou et al. [5] used response surface methodology (RSM) and physical test verification to optimize a large-diameter nozzle suitable for loose coal seam applications. Cui et al. [6] studied the external flow field of two different diameters of premixed abrasive water jet nozzles by means of numerical simulations. According to the liquid-solid two-phase flow theory inside a cone-shaped nozzle, Li et al. [7] conducted a numerical simulation study of the internal flow field of a nozzle. Shen [8] designed five different structures of nozzles based on the main parameters of the nozzles and established a solid-liquid two-phase flow model. Jou [9] conducted an analytical study for the characteristics of the jet boundary layer. By using high-speed photographic techniques, Liao et al. [10] performed a comparative study of the jet structure and the rock-breaking characteristics. Guo et al. [11] carried out a

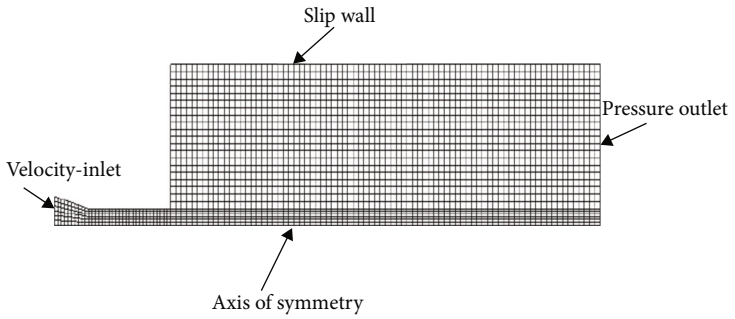

Figure 1: Modeling notation.

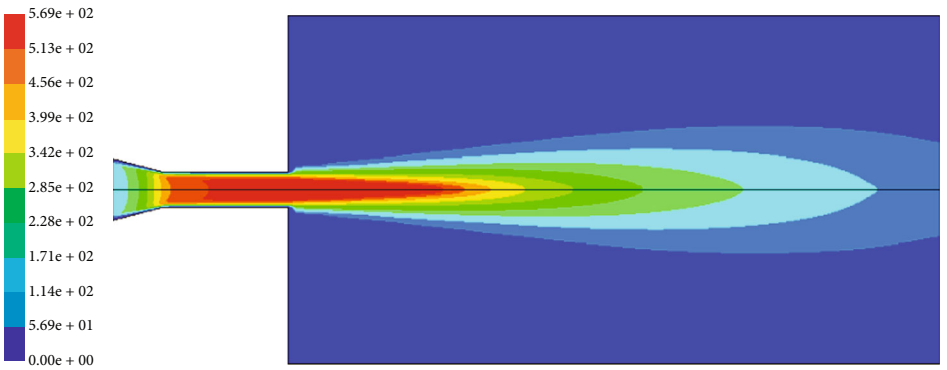

(a) Velocity contour

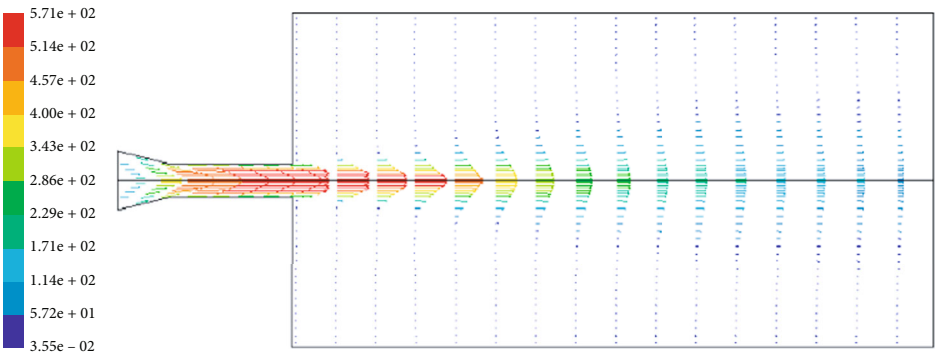

(b) Velocity vector

Figure 2: Velocity distribution of the water jet (m/s).

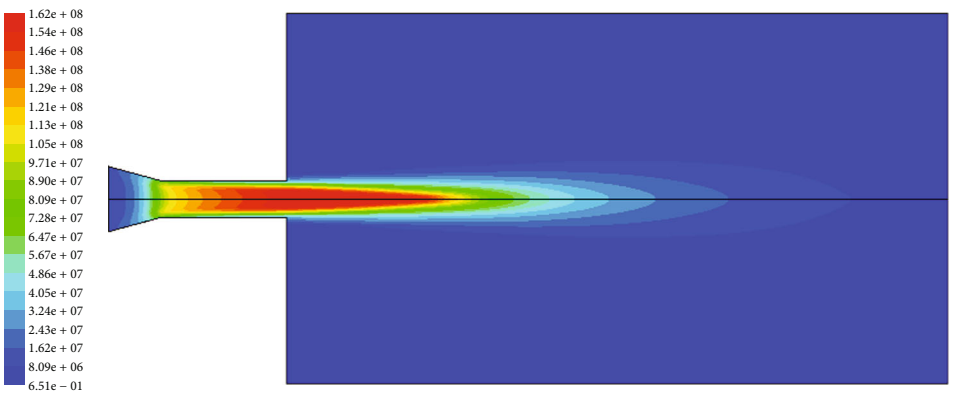

Figure 3: Dynamic pressure distribution of the water jet (Pa).

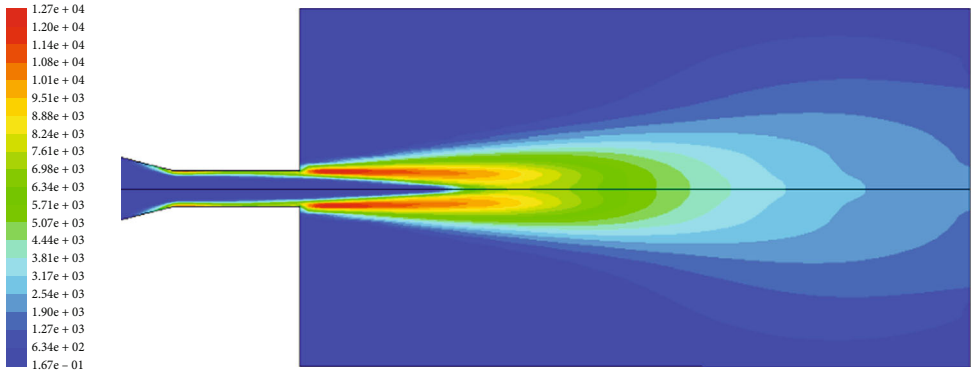

(a) Turbulent kinetic energy k

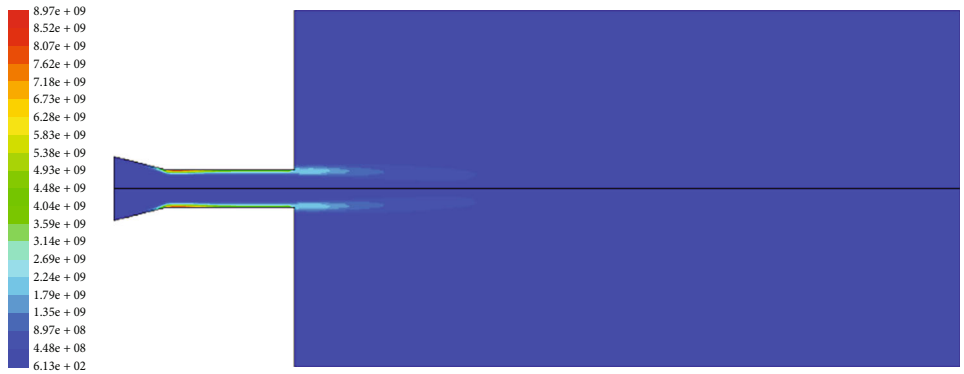

(b) The dissipation rate of turbulent kinetic energy ε

Figure 4: Turbulent kinetic energy distribution of the water jet.

numerical simulation study of the flow field of an abrasive water jet nozzle using two turbulence models. Kang [12] investigated the intermixing process of pure water jets, abrasives, and air by theoretical analysis and numerical simulation. Wang et al. [13] carried out the structural design of the nozzle and studied the gas-liquid two-phase flow field inside and outside the nozzle. Yang et al. [14] studied the relationship between the influencing factors of energy loss and the flow coefficient. Jiang et al. [15] conducted experiments with high-pressure water jet nozzles of different parameters for cutting coal samples of different hardness and derived the relationship between the nozzle parameters and the width and depth of the slotting and optimized the design of the slotting jet nozzle and the processing parameters. Han et al. [16] proposed a nozzle structure to generate self-oscillating jets and investigated the dynamic pressure distribution pattern inside the nozzle cavity. Gong et al. [17] studied a full-size self-oscillating pulse jet nozzle based on FLUENT simulation software and simulated a variety of operating conditions. Wang [18] researched the nozzle structure of multiphase flow by FLUENT numerical simulation software and explored the influence of nozzle geometric parameters on its internal flow field and proposed a nozzle structure with better cutting performance. Liao et al. [19, 20] derived the peak pressure, erosion volume, and effective target distance of the jet by means of a developed self-excited oscillating pulse nozzle. Zhang et al. [21, 22] studied the damage characteristics of gas-containing coal by experiment.

In summary, high-pressure water jet research methodologies are split into theoretical and experimental investigations; however, numerical simulation and experimental studies are not mutually verified. Based on this, this paper uses numerical simulation and field tests to investigate the structural properties of high-pressure water jets and the influence rule of nozzle parameters on water jets, with the goal of giving theoretical and practical guidance for hydraulic slotting methods.

2. The Effect of High-Pressure Water Jet Nozzle Parameters on the Jet Flow Field

2.1. Numerical Model. As illustrated in Figure 1, the model was created using the FLUENT software. The contraction angle of the model is 13°, the length of the contraction section is 10 mm, the length of the straight column section is 8 mm, the nozzle outlet diameter is 2 mm, and the nozzle inlet water pressure is 20 MPa. The quadrilateral grids are applied to numerical models, and a submerged water jet is used.

Figures 2(a) and 2(b) show the velocity distribution of the water jet and the distribution of velocity vector, respectively.

Figure 3 depicts the dynamic pressure distribution of the water jet. The dynamic pressure contour distribution of the water jet is similar to the velocity contour distribution of the water jet. At a distance from the nozzle, the effect area

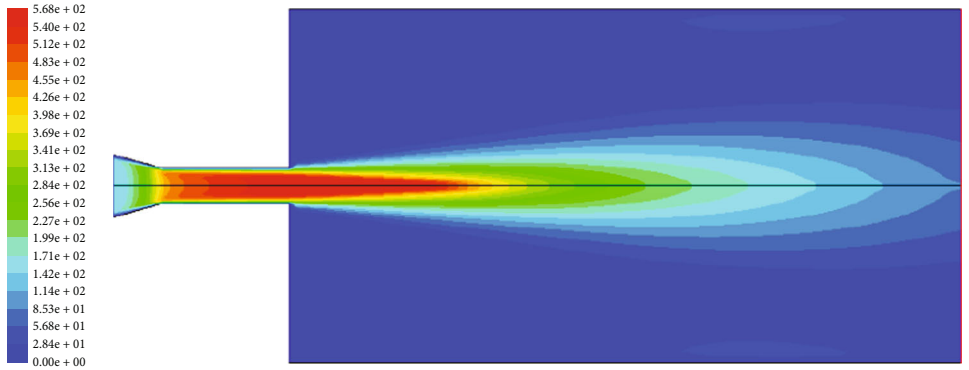

(a) The contraction angle is 30°

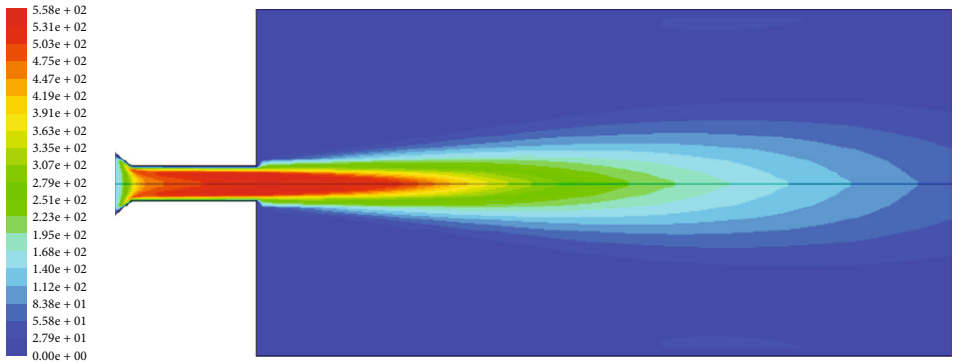

(b) The contraction angle is 60°

Figure 5: Velocity distribution of the water jet (m/s).

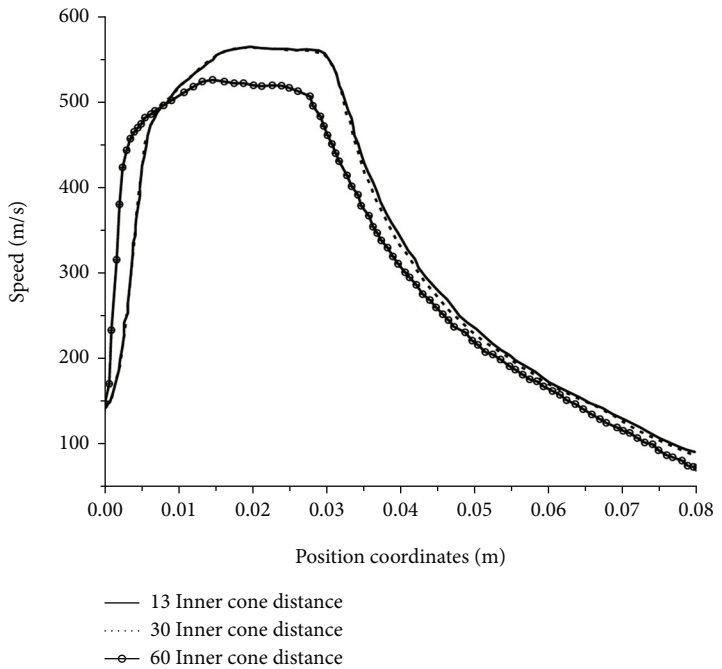

Figure 6: Velocity distribution of the water jet on the central axis.

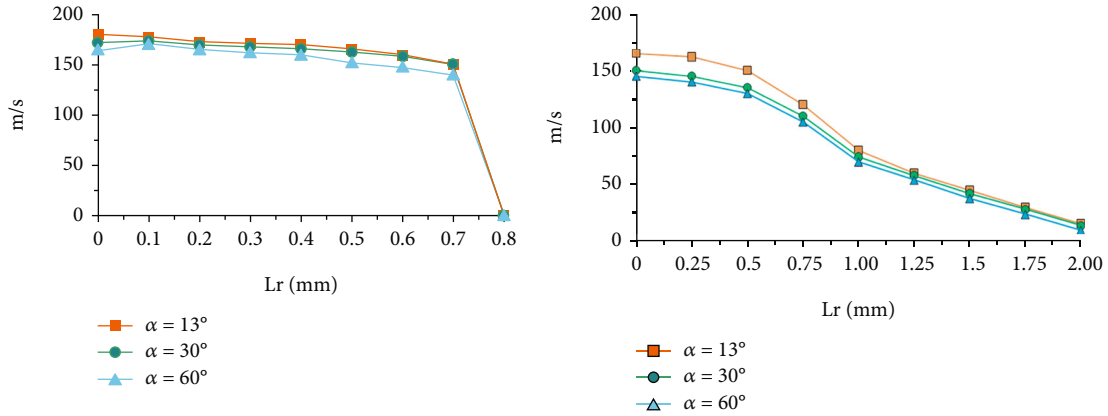

(a) The distance from the nozzle outlet is 0

(b) The distance from the nozzle outlet is 5 d

Figure 7: Velocity distribution of the water jet on the vertical axis.

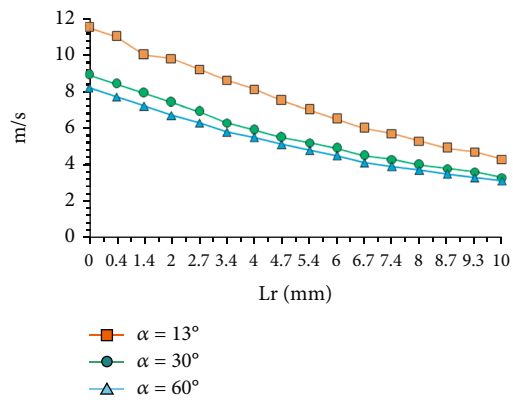

Figure 8: Pressure distribution of the water jet on the central axis.

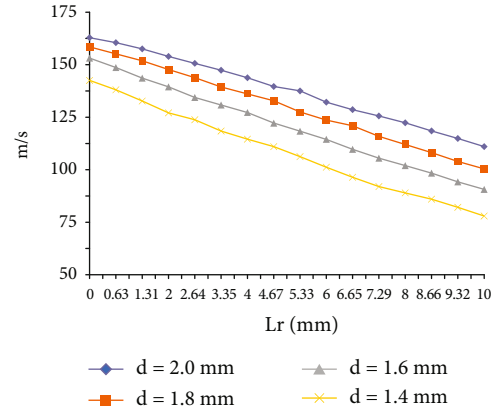

Figure 9: Velocity distribution of the water jet on the central axis.

of the dynamic pressure of the water jet is smaller than that of the velocity of the water jet.

The turbulent kinetic energy k distribution of the water jet and the dissipation rate of turbulent kinetic energy ε are shown in Figures 4(a) and 4(b). The areas of higher turbulent kinetic energy are inside the nozzle, at the junction of the constriction and straight column sections. Outside the nozzle, the areas of higher turbulent kinetic energy are on either side of the core, and the areas of lower turbulent kinetic energy are within the core, which is consistent with the turbulent flow conditions seen in field applications. The areas of higher turbulent kinetic energy dissipation are at the constriction angle, the inner wall of the straight column section, and the nozzle outlet.

2.2. The Effect of Nozzle Constriction Angle on the Flow Field. Figures 5(a) and 5(b) show the velocity distribution of the water jet for contraction angles of 30° and 60°, with all other parameters constant.

According to the theoretical formula, when the nozzle inlet water pressure is $p_{in} = 20$MPa, the theoretical velocity of the nozzle outlet is $v_t = 200$ m/s. When $\alpha = 13°$, the actual velocity of the nozzle outlet is $v = 187$ m/s, then the velocity coefficient is $c_v = v/v_t = 0.94$. When $\alpha = 30°$, the actual velocity of the nozzle outlet is $v = 180$ m/s and $c_v = v/v_t = 0.9$. When $\alpha = 60°$, the actual velocity of the nozzle outlet is $v = 170$ m/s and $c_v = v/v_t = 0.89$.

Figure 6 shows the velocity distribution of the water jet on the central axis for 13°, 30°, and 60° contraction angles. With contraction angles of 13° and 30°, the velocity distribution on the central axis is essentially the same. With the contraction angle of 60°, the velocity distribution on the central axis is significantly lower. Meanwhile, the nozzle at the cone angle has a large velocity loss, and the velocity of the water jet in the straight column section is unbalanced and the velocity is the lowest. The dynamic pressure in the core area is the lowest. As a consequence, the nozzle performs best at a contraction angle of 13°.

With contraction angles of 13°, 30°, and 60°, the velocity distribution of the water jet on the vertical axis whose distance from the nozzle outlet is 0 and 5 d is shown in Figures 7(a) and 7(b).

When the distance from the nozzle outlet is 0, as the distance from the axis increases, the velocity of water jet decreases from slowly to rapidly. To the inner wall of the nozzle, the velocity of water jet quickly becomes 0. At the same location, the smaller the contraction angle, the bigger the velocity of the water jet. When the contraction angle is 13°, the velocity of water jet is maximum.

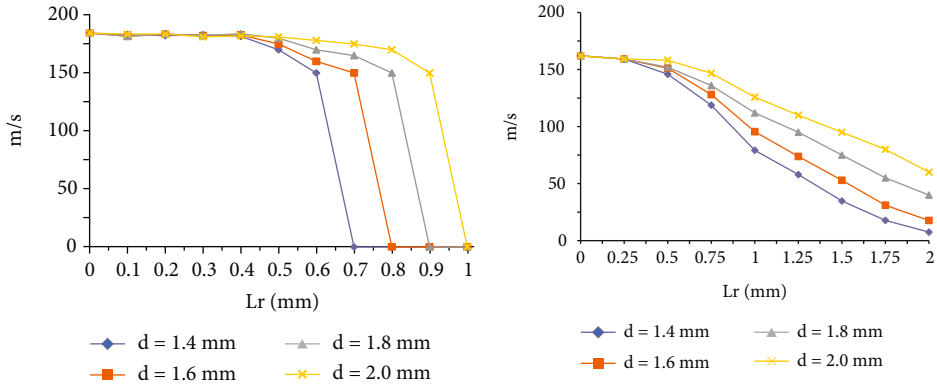

(a) The distance from the nozzle outlet is 0

(b) The distance from the nozzle outlet is 5 d

Figure 10: Velocity distribution of the water jet on the vertical axis.

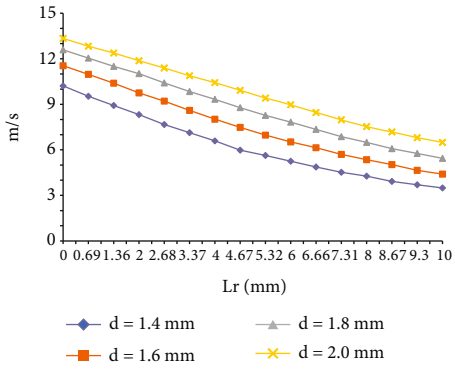

Figure 11: Pressure distribution of the water jet on the central axis.

When the distance from the nozzle outlet is 5 d, the velocity of the water jet gradually decreases as the distance from the axis increases. When the distance from the axis is less than 1.12 mm, at the same position, the smaller the contraction angle, the bigger the velocity of the water jet. When the distance from the axis is more than 1.12 mm, at the same position, the smaller the contraction angle, the smaller the velocity of the water jet, and the velocity is relatively small at this point.

Figure 8 depicts the pressure distribution of water jet on the central axis for contraction angles of 13°, 30°, and 60°. The pressure of the water jet decreases as the distance from the nozzle increases after it leaves the nozzle outlet. The pressure distribution on the central axis is substantially higher when the contraction angle is 13°. When the contraction angle is 30° or 60°, the pressure distribution on the central axis is identical. When the contraction angle is 13°, the water jet has the highest dynamic pressure.

2.3. The Effect of Nozzle Outlet Diameters on the Flow Field. Figure 9 shows the velocity distribution of the water jet on the central axis for nozzle outlet diameters of 1.4 mm, 1.6 mm, 1.8 mm, and2.0 mm, with all other parameters constant.

With nozzle outlet diameters of 1.4 mm, 1.6 mm, 1.8 mm, and 2.0 mm, the velocity distribution of the water jet on the vertical axis whose distance from the nozzle outlet is 0 and 5 d is shown in Figures 10(a) and 10(b).

When the distance from the nozzle outlet is 0, as the distance from the axis increases, the velocity of water jet decreases from slowly to rapidly. To the inner wall of the nozzle, the velocity of water jet quickly becomes 0. At close proximity to the nozzle outlet, the velocity of the water jet is relatively close. When the distance from the nozzle outlet is more than 0.5 mm, the velocity of the water jet varies greatly; at the same location, the larger the outlet diameter, the slower the velocity decay.

When the distance from the nozzle outlet is 5 d, the velocity of the water jet gradually decreases as the distance from the axis increases. At the same position, the velocity of the water jet increases as the nozzle outlet diameter increases. The larger outlet velocity allows for a larger diameter water jet with greater energy.

With nozzle outlet diameters d of 1.4 mm, 1.6 mm, 1.8 mm, and 2.0 mm, the pressure distribution of the water jet on the central axis is shown in Figure 11. The pressure of the water jet decreases as the distance from the nozzle increases after it leaves the nozzle outlet. At the same position, the velocity of the water jet increases as the nozzle outlet diameter increases. When the nozzle outlet diameter is 2.0 mm, the velocity of the water jet is the largest.

2.4. The Effect of Straight Column Section Lengths on the Flow Field. Figures 12(a) and 12(b) show the velocity distribution and the dynamic pressure distribution of the water jet on the central axis for straight column section lengths of 4 mm (2D), 8 mm (4D), 12 mm (6D), and 24 mm (12D), with all other parameters constant.

When the straight column section lengths are different, the velocity distribution and the dynamic pressure distribution of the water jet on the central axis are the same. At the same position, the velocity of the water jet and dynamic pressure increase as the length of the straight column section increases and reaches the limit state when the length of straight column section is 24 mm. For water jets in the core area, the length of the core area and the length of the straight column section are negatively correlated. When the length of

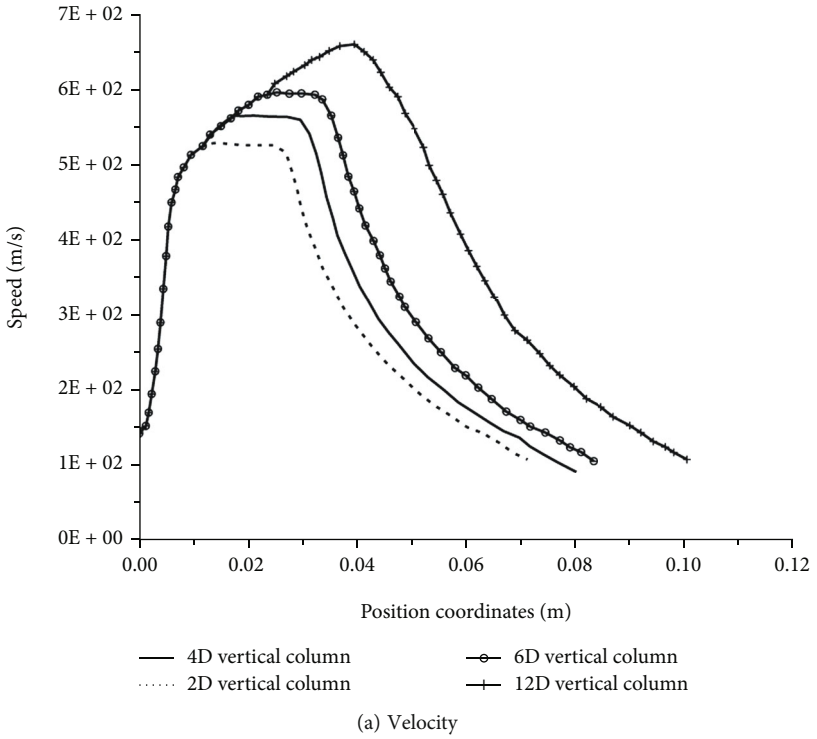

(a) Velocity

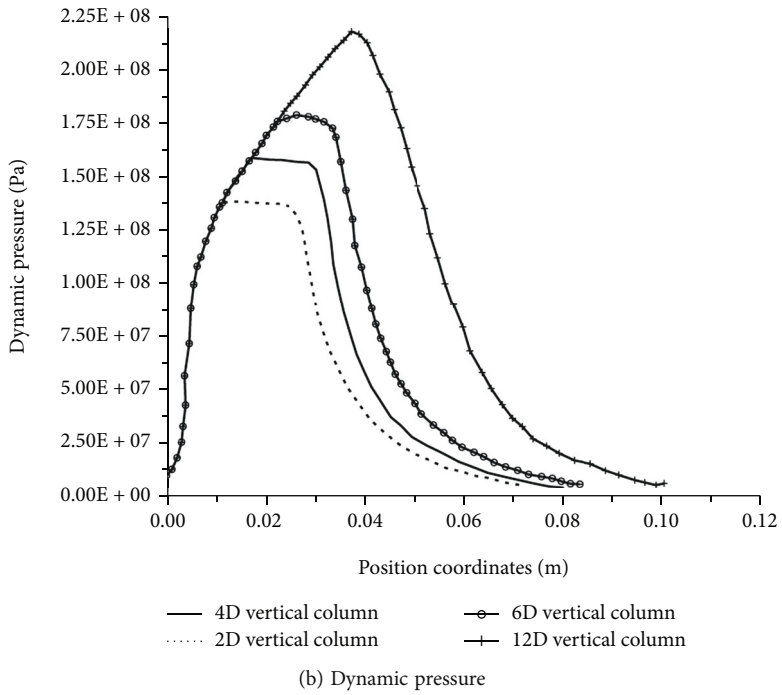

(b) Dynamic pressure

Figure 12: The distribution of the water jet on the central axis.

the straight column section is 4 mm, the nozzle has the largest core area.

In conclusion, when determining the length of the straight column section, both the length of the straight column section and the variation in the velocity of the water jet and dynamic pressure should be considered. As a result, the demand can be met by selecting a 4D or 6D straight column section length.

3. Mathematical Model of Nozzle Outlet Water Velocity

Other parameters stay constant when the model contraction angle is altered. Figure 13 shows the relationship between the nozzle outlet velocity of the water jet and contraction angle for nozzle contraction angles of 0°, 20°, 50°, 90°, 120°, and 180°, respectively.

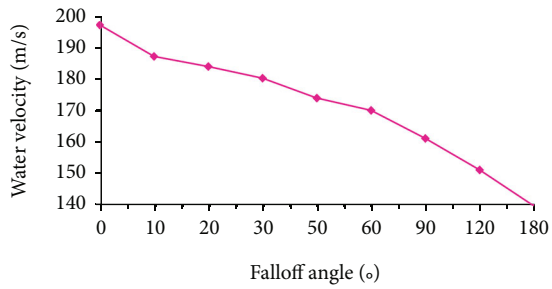

Figure 13: Relationship between the nozzle outlet velocity of the water jet and contraction angle.

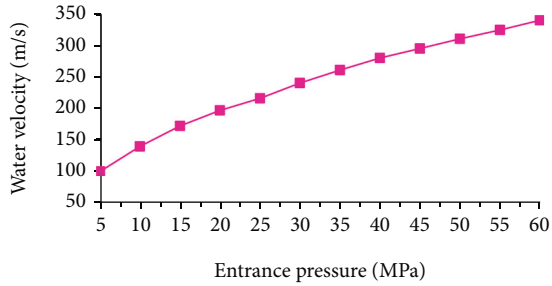

Figure 14: Relationship between the nozzle outlet velocity of the water jet and the nozzle inlet water pressure.

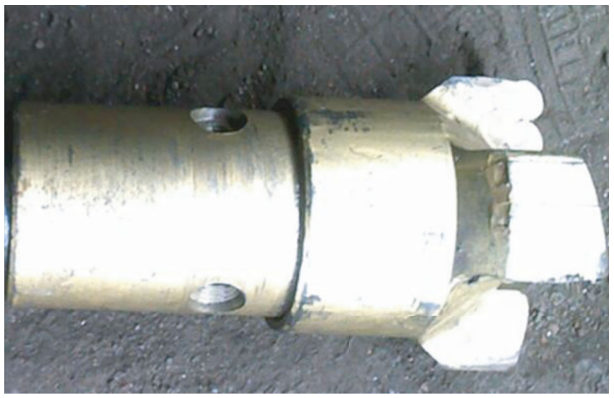

Figure 15: Water jet cutting bit.

Table 1: Geometric parameters of the nozzles.

Nozzle number	Nozzle outlet diameter d (mm)	Contraction angle (°)	Contraction section length L (mm)	Straight column section length l (mm)
1	1	13°	5	4
2	2	13°	10	8
3	3	13°	12	16

Table 2: Test result.

Nozzle number	Depth of the hole (mm)	Width of the hole (mm)	Volume of the hole (m^3)
1	805	16	0.0002
2	642	25	0.0004
3	374	32	0.00038

The relationship between water jet velocity and contraction angle at the nozzle outlet can be obtained by fitting:

$$v_0 = 44.159p^{0.5}. \quad (1)$$

In the formula, v is the nozzle outlet velocity of the water jet (m/s), m is constant, and α is the contraction angle (°).

Other parameters stay constant when the model inlet water pressure is altered. When the contraction angle is 0°, Figure 14 shows the relationship between the nozzle outlet velocity of the water jet and nozzle inlet water pressure for nozzle inlet water pressures of 5 MPa, 10 MPa, 15 MPa, 30 MPa, 40 MPa, 50 MPa, and 60 MPa, respectively.

The relationship between the nozzle outlet velocity of the water jet and the nozzle inlet water pressure can be obtained by fitting:

$$v_0 = 44.159p^{0.5}. \quad (2)$$

From equation (1), when the contraction angle is 0°, m equals to the nozzle outlet velocity of the water jet v_0, that is,

$$m = 44.159p^{0.5}. \quad (3)$$

Substitution into equation (1) yields

$$v = 44.159p^{0.5}e^{-0.0019\alpha}. \quad (4)$$

The geometric properties of the nozzle indicate that

$$\alpha = 2 \arctan \frac{D-d}{2L}. \quad (5)$$

Substitution into equation (4) yields

$$v = 44.159p^{0.5}e^{-0.0038 \arctan ((D-d)/2L)}. \quad (6)$$

In the formula, v is the nozzle outlet velocity of the water jet (m/s), p is the nozzle inlet water pressure (MPa) (5 MPa < p < 60 MPa), a is the nozzle outlet diameter (mm), D is the nozzle inlet diameter (mm), and L is the length of the straight column section (mm).

4. Field Verification of High-Pressure Water Jet Nozzle Parameters

Figure 15 shows the water jet cutting bit used in the test mine, which is a drilling-cutting integrated bit. Three nozzles, each at 120°, are distributed in the same plane perpendicular to the drill pipe. Due to issues with the geometry of

the nozzle settings, the hydraulic slotting is ineffective in breaking the coal.

To optimize the geometric parameters of the hydraulic slotting nozzle, a high-pressure water jet breaking coal field test was performed. According to fluid mechanics theory, the geometric parameters of the three nozzles of the drilling-cutting integrated bit are the same and are arranged centrally symmetrically. Thus, verifying the single nozzle is sufficient. Table 1 displays the geometric parameters of the nozzles.

The coal breaking time is 1 minute, and the pump pressure is set at 30 MPa. The depth, width, and volume of the holes created by the impact of three nozzles were measured, and the test results are displayed in Table 2.

With the cutting depth and width for the middle level and the maximum hole volume, the no. 2 nozzle was used, which is superior to the nozzle used in the mine to break the coal effect. All in all, the geometric parameters of the mine's hydrodynamic slotting nozzle are optimized as follows: outlet diameter of 2 mm, length of contraction section of 10 mm, length of straight column section of 8 mm, and contraction angle of 13°.

5. Conclusion

The influence rule of high-pressure water jet structure characteristics and nozzle parameters on the effect of hydraulic slotting was studied by numerical simulation and field test. The main conclusions are as follows:

(1) The velocity of the water jet in the contraction section is constantly increasing, and the water jet in the straight column section is relatively stable. The velocity of the water jet outside the compact section gradually decreases until it reaches 0 m/s. The velocity, dynamic pressure, and kinetic energy of the water jet on the parallel axis increase and subsequently decrease as the distance from the nozzle increases. The velocity, dynamic pressure, and kinetic energy of the water jet at the axis point are the highest. The velocity, dynamic pressure, and kinetic energy of the water jet on the vertical axis all decrease as the distance from the axis increases. The velocity, dynamic pressure, and kinetic energy of the water jet on the vertical axis begin to decay sooner as the distance from the nozzle increases, the decay rate reduces, and the range increases. The effect area of the kinetic pressure of the water jet is smaller than that of the velocity

(2) The distribution rules of water jet velocity and dynamic pressure on the central and vertical axes are obtained for contraction angles of 13°, 30°, and 60°, and it is determined that the nozzle with a contraction angle of 13°is the most effective. The distribution rules of water jet velocity and dynamic pressure on the central and vertical axes are obtained for nozzle outlet diameters of 1.4 mm, 1.6 mm, 1.8 mm, and 2.0 mm, and it is found that the nozzle with a 2.0 mm outlet diameter is proven to be the most effective. The distribution rules of water jet velocity and dynamic pressure on the central and vertical axes are obtained for straight column section lengths of 4 mm, 8 mm, 12 mm, and 24 mm, and it is established that the nozzles with straight column section lengths of 8 mm and 12 mm are available to meet the requirements

(3) The relationship between the nozzle contraction angle gradient, the inlet water pressure, and the nozzle outlet water velocity is discovered. A mathematical model of the nozzle outlet water velocity of the water jet is established. The depth, width, and volume of the hole generated by the nozzle impact are employed as indications for inquiry; the following are the findings of nozzle geometry parameter optimization based on field measurements: outlet diameter of 2 mm, length of contraction section of 10 mm, length of straight column section of 8 mm, and contraction angle of 13°

Data Availability

The data used to support the findings of this study are available from the corresponding author upon request.

Conflicts of Interest

The authors declare that they have no conflicts of interest.

Authors' Contributions

Beifang Gu contributed to the conception of the study, performed the data analyses, and wrote the manuscript. Ruili Hu helped perform the paper revision process with constructive discussions. Longkang Wang performed the numerical simulation. Guanchao Xu helped perform the numerical simulation.

Acknowledgments

This study is supported by the North China University of Water Resources and Electric Power Scientific Research Launching Project for High-Level Talents.

References

[1] Y. Guolai, Z. Wenhui, and L. Fei, "Flow field simulation of high pressure water jet nozzle based on FLUENT," *Journal of Lanzhou University of Technology*, vol. 2, pp. 49–52, 2008.

[2] M. Fei and Z. Wenming, "Numerical simulation of internal flow field of water jet nozzle with orifice expansion," *Journal of University of Science and Technology Beijing*, vol. 6, pp. 576–580, 2006.

[3] Z. Shaojun, H. Shushan, L. Guoyong, Z. Dongmei, Y. Chunyan, and L. Rong, "Layout parameters of controlled cooling nozzle for seamless steel pipe based on Fluent," *Journal of University of Science and Technology Beijing*, vol. 1, pp. 123–127, 2010.

[4] G. Zhaolong, L. Yiyu, Z. Weiqin, X. Binwei, Z. Yanoping, and T. Jiren, "Numerical simulation and experimental study of hydraulic sandblasting perforating nozzle," *Journal of Zhengzhou University (Engineering Edition)*, vol. 3, pp. 119–123, 2011.

[5] Z. Quanle, L. Boquan, Z. Chunshan et al., "Robust optimization of drilling-cutting integrated nozzle based on response surface method," *Journal of China University of Mining and Technology*, vol. 6, pp. 905–910, 2013.

[6] C. Junkui, Z. Jun, L. Guowei, G. Renning, and W. Chunxiao, "Simulation and experiment of the external flow field of the pre-mixed abrasive water jet nozzle," *Journal of China Coal Society*, vol. 3, pp. 410–414, 2009.

[7] L. Deyu, W. Haijin, and W. Chunli, "Numerical study on characteristics of hydraulic cutting nozzle in coal seam," *Journal of China Coal Society*, vol. 4, pp. 686–690, 2010.

[8] S. Juan, *Design of High-Pressure Water Jet Nozzle and Its Structural Optimization*, Soochow University, 2014.

[9] M. Jou, "Analysis of the stability of water-jet cutting with linear theory," *Journal of Materials Processing Technology*, vol. 104, no. 1-2, pp. 17–20, 2000.

[10] L. Hualin, L. Gensheng, L. Jingbin, and N. Jilei, "Analysis of flow field characteristics of radial horizontal drilling straight-rotating mixed jet nozzle," *Journal of China Coal Society*, vol. 11, pp. 1895–1900, 2012.

[11] G. Renning, W. Ruoxu, and C. Yang, "Numerical simulation of flow field of abrasive water jet nozzle," *Chemical Industry and Engineering Progress*, vol. S1, pp. 443–446, 2009.

[12] K. Lei, *Study on geometry and performance of high pressure abrasive water jet nozzle*, Yanshan University, 2015.

[13] W. Chaohui, L. Zhenfang, and Y. Xiqiao, "Design and numerical simulation of a new air-soluble jet nozzle," *Journal of Basic Science and Engineering*, vol. 3, pp. 616–624, 2014.

[14] Y. Yousheng, Z. Jianping, and N. Songlin, "Study on energy loss of nozzles in water jet system," *Chinese Journal of Mechanical Engineering*, vol. 49, no. 2, pp. 139–145, 2013.

[15] J. Wenzhong, L. Baodong, W. Yaofeng, and Y. Yongin, "Experimental study on slit parameters of non-submerged high-pressure rotating water jet nozzle," *Safety in Coal Mines*, vol. 10, pp. 1–3, 2009.

[16] H. Jian, L. Jing, W. Hui, M. Fei, and C. Tengfei, "Signal detection method in oscillation cavity of self-vibration jet nozzle," *Journal of Engineering Science*, vol. 9, pp. 1191–1197, 2015.

[17] G. Yongjun, G. Chen, H. Jiaoyi, and Z. Zengmeng, "Full size structure optimization of pulsed jet nozzle based on Fluent," *Journal of Chinese Hydraulics & Pneumatics*, vol. 11, pp. 32–35, 2014.

[18] W. Rongjuan, *Study on Optimization of Micro Abrasive Water Jet Nozzle*, Xihua university, 2011.

[19] L. Zhenfang, T. Chuanlin, and Z. Fenghua, "Experimental study on self-excited oscillation pulsed jet nozzle," *Journal of Chongqing University (Natural Science Edition)*, vol. 2, pp. 28–32, 2002.

[20] L. Zhenfang and T. Chuanlin, "Theoretical analysis of self-excited oscillation pulse jet nozzle," *Journal of Chongqing University (Natural Science Edition)*, vol. 2, pp. 24–27, 2002.

[21] M. Zhang, M. Lin, H. Zhu, D. Zhou, and L. Wang, "An experimental study of the damage characteristics of gas-containing coal under the conditions of different loading and unloading rates," *Journal of Loss Prevention in the Process Industries*, vol. 55, pp. 338–346, 2018.

[22] M. Zhang, Z. Zhang, D. Zhang et al., "Study on pore and fissure structure characteristics of deep soft coal rock," *Geofluids*, vol. 2021, 13 pages, 2021.